Chemistry Europe Amplifying Great Science

Chemistry Europe
European Chemical Societies Publishing

Stop by our **booth #3**

EuChemS Chemistry Congress
28 August to 1 September 2022 · LISBON.PT

Chemistry Europe Symposium
Monday, August 29, 9:15 – 12:30
Room #9

- We will celebrate the 10th anniversaries of *ChemistryOpen* and *ChemPlusChem*
- Mark the launch of *Chemistry-Methods* and *Analysis & Sensing*
- And introduce the redesign of *ChemistryViews* on a new platform

Join us for five fascinating talks by top scientists

Célia Fonseca-Guerra
Vrije Universiteit Amsterdam

Francesco Ricci
Rome Tor Vergata

Javier García Martínez
Universidad de Alicante
Current President of IUPAC

Anat Milo
Ben Gurion University

Ramón Martínez Mánez
Universitat Politècnica de Valènzia

We look forward to seeing you in Lisbon

chemistry-europe.org

EurJOC
European Journal of Organic Chemistry

Research Article
doi.org/10.1002/ejoc.202101357

Chemistry Europe
European Chemical Societies Publishing

www.eurjoc.org

VIP *Very Important Paper*

Special Collection

Synthesis of a Substituted [10]Cycloparaphenylene through [2+2+2] Cycloaddition

Jannis Volkmann,[a, b] Daniel Kohrs,[a, b] Felix Bernt,[a, b] and Hermann A. Wegner*[a, b]

Herein, we report the synthesis and investigation of a substituted [10]cycloparaphenylene (CPP) incorporating a diethylphthalane unit. An efficient strategy relying on a symmetric built-up starting with propargyl ether as [2+2+2] cycloaddition precursor was developed. The straightforward synthesis required overcoming unexpected obstacles within the [2+2+2] cycloaddition, protection and aromatization. These results give valuable insights for accessing CPPs with highly substituted subunits. Finally, a seven-step synthesis with an overall yield of 8% provided the target nanoring, including good to excellent yields for the critical macrocyclization and aromatization. The synthesized nanohoop exhibits a hypsochromic shift in fluorescence and absorption, compared to the unsubstituted [10]CPP. This observation is proposedly caused by an increased torsion angle between the bivalent substituted phenyl moieties and the adjacent units.

Introduction

Cycloparaphenylenes (CPPs), the shortest cutout of an armchair carbon nanotube, attract attention in the fields of organic synthesis, as well as molecular materials:[1,2] The distortion of their radially oriented π-systems in these nanohoops result in unique optoelectronic as well as supramolecular properties, which are not only dependent on the ring size, but also on the substituents.[3] The extraordinary structure of these nanorings makes the development of new syntheses still an ambitious task. Hence, general access to CPPs with a high degree of substitution represents still an unsolved challenge. In recent years, different strategies were explored to introduce manifold substituents and substitutional pattern to CPPs (Figure 1).[2,4,5–8] Two major approaches can be distinguished: The post functionalization of non-substituted CPPs[9–12] and the introduction of substituents within the first building blocks.[13–15] The first principally offers the largest flexibility as unsubstituted CPPs are modified in the last step(s) of their synthesis. However, this method is restricted by its low selectivity and suffers from a low substrate tolerance (*i.e.* ring size).[11] Besides this, the accessible degree and pattern of substitution is still strongly limited. Therefore, this approach is not practical to access a broad variety of functionalized nanohoops.

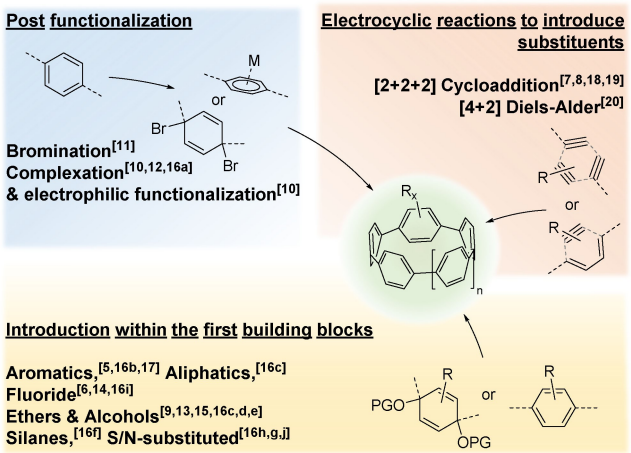

Figure 1. Summary of strategies to access for substituted CPPs, classified by their synthetic methodology.[5–20]

The introduction of substituents within the first steps of the synthesis, on the other hand, is restricted by the requirement, that the introduced substituents have to tolerate every applied reaction condition within the synthesis. This drawback can be partially circumvent by using a dummy, which tolerates these conditions and can be easily transferred into the desired functionality.[17] Nevertheless, this approach is again limited to specific substitution pattern and functionalities.

An alternative to these approaches is the introduction of substituents at a more advanced stage of the synthesis. Here, electrocyclic reactions,[20] as well as transition metal-catalyzed [2+2+2] cycloaddition reactions (CA) have proven their feasibility.[8,18,19] In general, the [2+2+2] CA is a highly efficient method to synthesize substituted aromatic rings in a regioselective fashion.[21] This methodology showed its potential in the

[a] *J. Volkmann, D. Kohrs, F. Bernt, Prof. Dr. H. A. Wegner*
Institute of Organic Chemistry,
Justus Liebig University Giessen
Heinrich-Buff-Ring 17, 35392 Giessen, Germany
E-mail: hermann.a.wegner@org.chemie.uni-giessen.de
https://www.uni-giessen.de/fbz/fb08/Inst/organische-chemie/Wegner
[b] *J. Volkmann, D. Kohrs, F. Bernt, Prof. Dr. H. A. Wegner*
Center for Material Research (ZfM/LaMa),
Justus Liebig University Giessen
Heinrich-Buff-Ring 16, 35392 Giessen, Germany
https://www.uni-giessen.de/fbz/zentren/lama/AGOrdner/personen/personen-layouts/q-z/wegner_hermann_layout

Supporting information for this article is available on the WWW under https://doi.org/10.1002/ejoc.202101357

Part of the "Carbon Allotropes" Special Collection.

Research Article
doi.org/10.1002/ejoc.202101357

preparation of substituted CPPs with either twofold,[7] or fourfold[8] functionalized phenyl units. Tanaka and coworkers, as well as our group exploited the strength of this reaction for the synthesis of substituted CPPs, introducing different functionalities, such as esters, ethers, aliphatic and aromatic side chains (Figure 1).[7,8] Furthermore, highly complex structural motifs such as a Möbius-shaped nanoring has been accessed via the [2+2+2] CA.[22]

In 2014, our group realized the incorporation of diethylphthalane units in [8]CPPs.[8] The steric demand of the annulated ring systems and the two substituents on the opposite side of the phenyl unit led to a significant increase in the torsion angle with their neighboring rings. As a consequence, the extinction coefficient decreased significantly, while the absorption maximum λ_{max} was hypsochromically shifted. This large torsion angle, as well as the tetravalent substitution pattern are of particular interest as design elements to control the optoelectronic and non-covalent interaction properties of these nanohoops. Even though the developed synthesis furnished a variety of novel, diverse [8]CPPs, the efficiency to access these substitution pattern for further use and investigation has to be improved.

Results and Discussion

Synthesis

In view of the drawbacks of the above discussed synthesis of substituted [8]CPPs *via* [2+2+2] CA, the new strategy towards such valuable tetra-substituted [10]CPP **1** was designed. By slicing the CPP in two equal parts, two symmetric five-membered building blocks (Scheme 1, **4** and **3**) would be obtained as precursors for a strain-reduced macrocyclic precursor **2**. While the unsubstituted building block **4** can be synthesized *via* a literature known procedure,[23] the substituted coupling partner **3** should be accessible *via* a [2+2+2] CA with 3-hexyne (**7**). This reaction could either be performed in the completing step of the building block synthesis towards **3** (path A), or one step in advance, forming a three-membered building block **5** (path B). The former approach is preferable, as one protection step is sufficient, while the latter approach requires a successive two-step protection. Further, only a bulky protecting group is suitable in path B to obtain a *syn*-selectivity within the formation of **3**. However, in path A the [2+2+2] CA is executed with a more sterically encumbered substrate, which might hamper the formation of the substituted core unit. Both described paths have their origin in the tethered diquinone derivative **8**. This substrate already contains the cyclohexadienes, which ensure the angular arrangement in the U-shaped

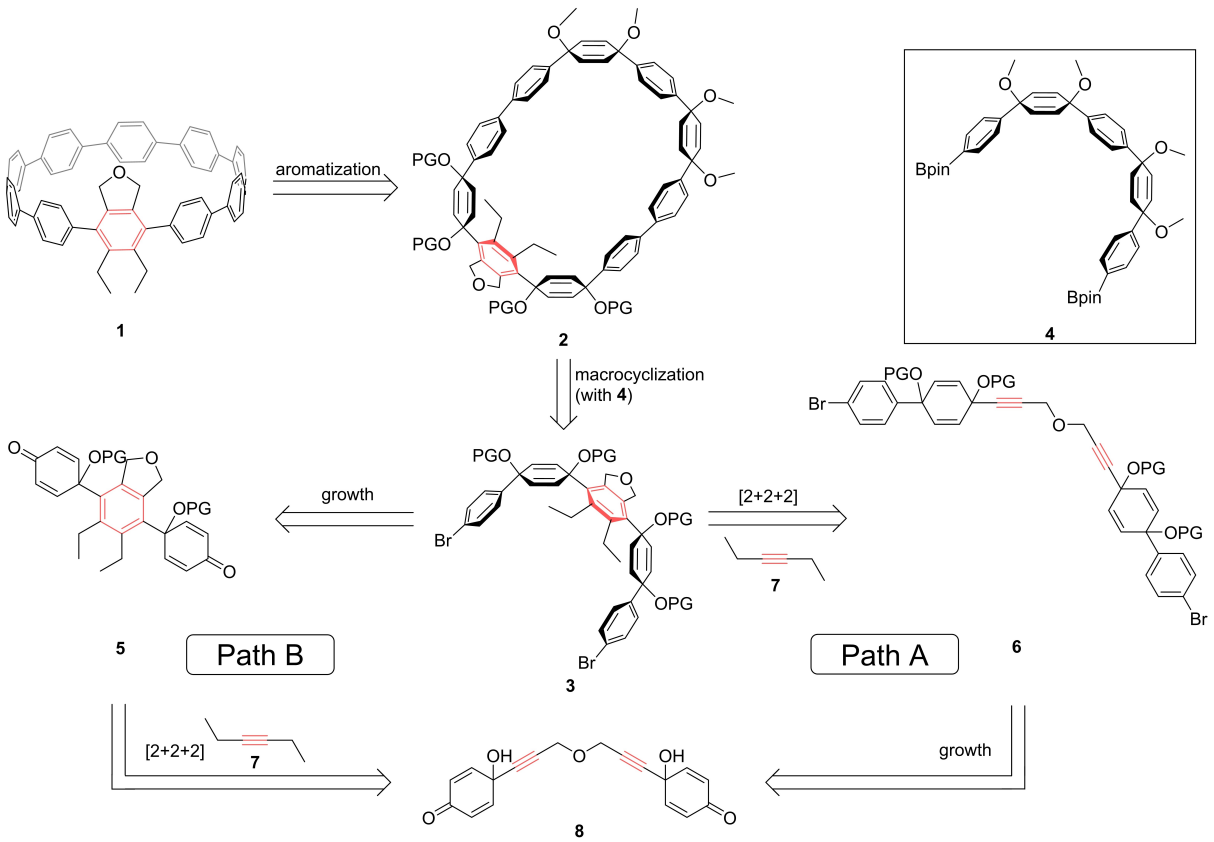

Scheme 1. Retrosynthetic perspective for the synthesis of target compound **1**. Two synthetic paths were followed, whereat the order of steps is changed, resulting in a difference in reactivity.

Research Article
doi.org/10.1002/ejoc.202101357

building block **3** enabling the formation of strain reduced macrocycle **2**. Dialkyne **8** is conveniently accessible from the commercially available propargyl ether **9** and 1,4-benzoquinone.

In the first step the propargyl ether **9** was deprotonated, followed by the addition of 1,4-benzoquinone forming the diketone **8** with a moderate yield of 37 % (Scheme 2). Increasing the amount of benzoquinone from 2.35 eq. to 3.52 eq. raised the yield to 53 %. The main side product was the mono addition product. However, increasing the amount of benzoquinone improved the ratio between double and single addition only marginally. In the following step, the extension of the building block was targeted (path A). Monolithiation of 1,4-dibromobenzene (**10**) and subsequent addition to the deprotonated diol **7** provided the tetraalcohol. As expected, one diastereomer was obtained in large excess.[24] At this point, it was not possible to remove traces of other diastereomers. Hence, the mixture of diastereomers was exposed directly to the protection toward tetra methyl ether **6-Me**. During a protection using NaH and iodomethane without an additive, no consumption of the diol was observed. A proton-deuterium exchange experiment proved the efficient deprotonation with sodium hydride (see Supporting Information Figure S1). Hence, the following nucleophilic attack of the sodium alcoholate emerged to be too hindered. Only by addition of 15-crown-5 in this protection the [2 + 2 + 2] precursor was accessed. The crown ether complexing the sodium increased the nucleophilicity of the alcoholate and thus enabled the completion of the ether synthesis of **6-Me**.

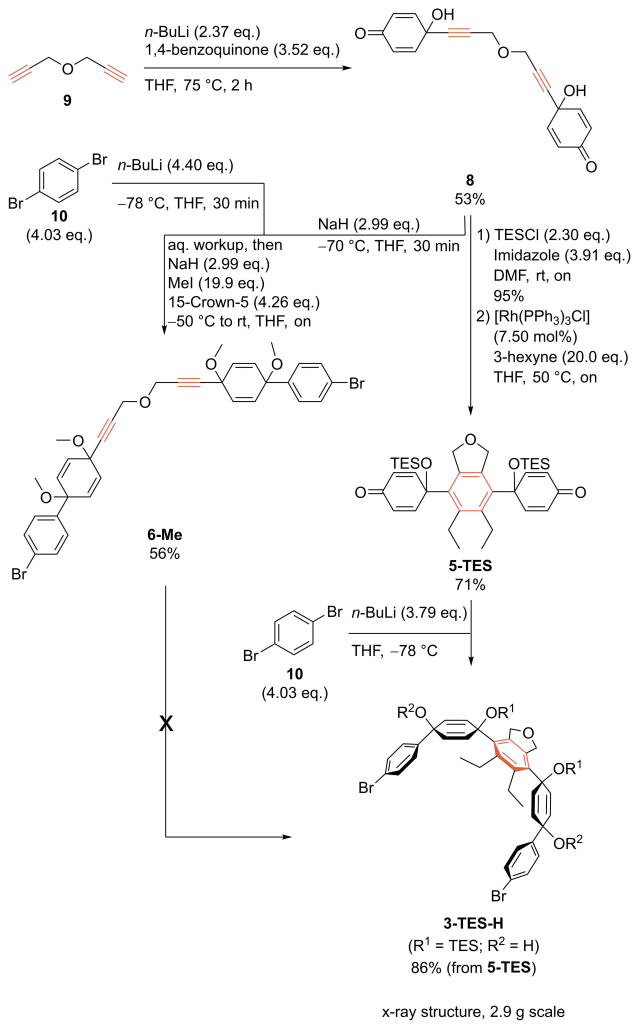

Scheme 2. Synthetic routes A & B toward five membered building block **3-TES-H**.

The following [2 + 2 + 2] CA was executed with 3-hexyne (**7**). Different temperatures and catalytic systems, as well as reactions in a microwave and a pressure tube were tested for this reaction (for further information see Supporting Information Table S1 and Table S2). However, the product was only obtained in traces. To elucidate this low reactivity, ^{1}H NMR experiments with stoichiometric and hyperstoichiometric amounts of Wilkinson's catalyst were performed (see Supporting Information Figure S3). The addition of a stoichiometric amount of the catalyst led to the formation of a new set of ^{1}H NMR signals with a ratio of 1 : 1 with respect to the signals of the starting material **6-Me**. Upon addition of a second equivalent of the catalyst, the signals of the starting material vanished. This result indicates the formation of an undesired 1 : 2 species of the dialkyne and the catalyst which did not proceed to the desired [2 + 2 + 2] cycloadduct.

As this strategy (path A) did not proceed as desired, the alternative pathway (path B) was followed. Here it was expected that the strongly reduced steric hindrance arising from the two *para*-bromophenyl groups should facilitate the [2 + 2 + 2] cycloaddition, more precisely the coordination and subsequent insertion of the third alkyne. Therefore, diol **8** was protected as di(triethylsilyl) ether in excellent yield. This protection prohibits undesired interactions of the hydroxyl group in the [2 + 2 + 2] cycloaddition, as well as ensures the *syn*-selectivity for the subsequent addition. Indeed, the [2 + 2 + 2] CA with 3-hexyne (**7**) and Wilkinson's catalyst (7.5 mol %) gave phthalane **5-TES** in 71 % yield. When the catalyst loading was lowered to 5.2 mol % the yield also decreased to 54 %. Next, 1,4-dibromobenzene (**10**) was lithiated and added to diketone **5-TES** providing the desired 5-membered building block **3-TES-H**. Suitable crystals for *X*-ray analysis of this key intermediate were obtained by layering a solution of **3-TES-H** in dichloromethane with *n*-pentane. The obtained solid-state structure shows a U-shape arrangement which is ideally oriented for the dimerization forming the ten-membered macrocycle **2** (Figure 2).

The remaining two hydroxyl groups in **3-TES-H** should be protected, either as their methyl or silyl ethers to prevent side reactions in the following steps. However, this protection emerged to be an unexpected challenge. Different strong bases, as well as protection agents were applied but the protection was not achieved. In the majority of cases, starting material was re-isolated, while harsh conditions led to decomposition. Proton-deuterium exchange ^{1}H-NMR experiments were performed, whereat no deprotonation with NaH was observed (see Supporting Information Figure S2). This finding is remarkable as there should be a difference in *p*Ka values of approximately 20–25 orders of magnitude between the tertiary alcohol and the corresponding acid of the applied base (based on the *p*Ka value

Research Article
doi.org/10.1002/ejoc.202101357

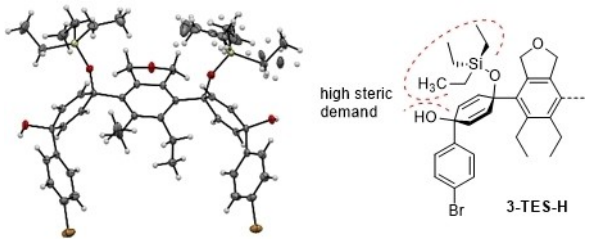

Figure 2. a) Solid state structure of the TES/OH-building block **3-TES-H** (ORTEP drawing, solvent molecules were omitted). b) Illustration of the proposed sterically shielding of the alcohol moieties by the bulky protecting group.

of known tertiary alcohols).[25] One explanation could be the strong steric hindrance of the tertiary alcohol with the large TES group in close proximity (Figure 2). The substituted phenyl ring thrusts the silyl ether toward the cyclohexadienes, where the bulky and flexible protecting group shields the free alcohol. Indeed, the crystal structure shows a proximity between protection group and the alcohols. Nevertheless, the hindrance to such a degree is surprising. The free and flexible rotation of the protecting group could increase this shielding drastically and therefore might explain the observed inertness. Despite the initial doubts the macrocyclization between substituted dibromide **3-TES-H** and non-substituted diboronic ester **4** was performed without protection using $Pd_2(dba)_3$ and the Buchwald ligand S-Phos (Scheme 3). The Suzuki coupling led to the macrocycle in an unexpectedly high yield of 31%. Deprotection with TBAF provided the mixed OH/OMe-macrocycle. For the final step, H_2SnCl_4, as well as sodium naphthalenide were tested to form the desired CPP **1**. While an aromatization with H_2SnCl_4 gave the product in traces, the product was not observed *via* single-electron reduction with sodium naphthalenide. This circumstance is presumably caused by the combination of cyclo-hexadienols, as well as their methyl ethers for the aromatization. In literature, the stannane-ate complex is majorly used for the aromatization of cyclohexadienols,[26] while, to the best of our knowledge, an aromatization with naphthalenide is only reported for the methyl ethers.

Based on this rationale, the all-methyl protected macrocycle **2-Me** was targeted. Therefore, the protection of the five-membered building block **3-TES-H** was resumed. The silyl ether was quantitatively cleaved with TBAF to the tetraalcohol. By applying NaH as base and iodomethane as the electrophile, the fourfold methyl protected building block **3-Me** was obtained in 81% over two steps. The fact, that this protection was successful, strengthens the assumption that the deprotonation of **3-TES-H** was sterically strongly hindered by the large silyl protecting group. With building block **3-Me** and non-substituted diboronic ester **4** in hand, again, a macrocyclization with similar conditions was executed, yielding the fully protected macrocycle in an even better yield of 46%. As expected, the aromatization with an excess of sodium naphthalenide led to the desired diethylphthalane incorporated [10]CPP **1**. In contrast to the previous aromatization attempts of macrocycle **2-TES-H**, the outcome was strongly improved to a yield of 70%. In total, an overall yield of 8% was achieved for this seven-step synthesis. This displays an exceedingly increase in yield compared to our previously reported synthesis of a similarly

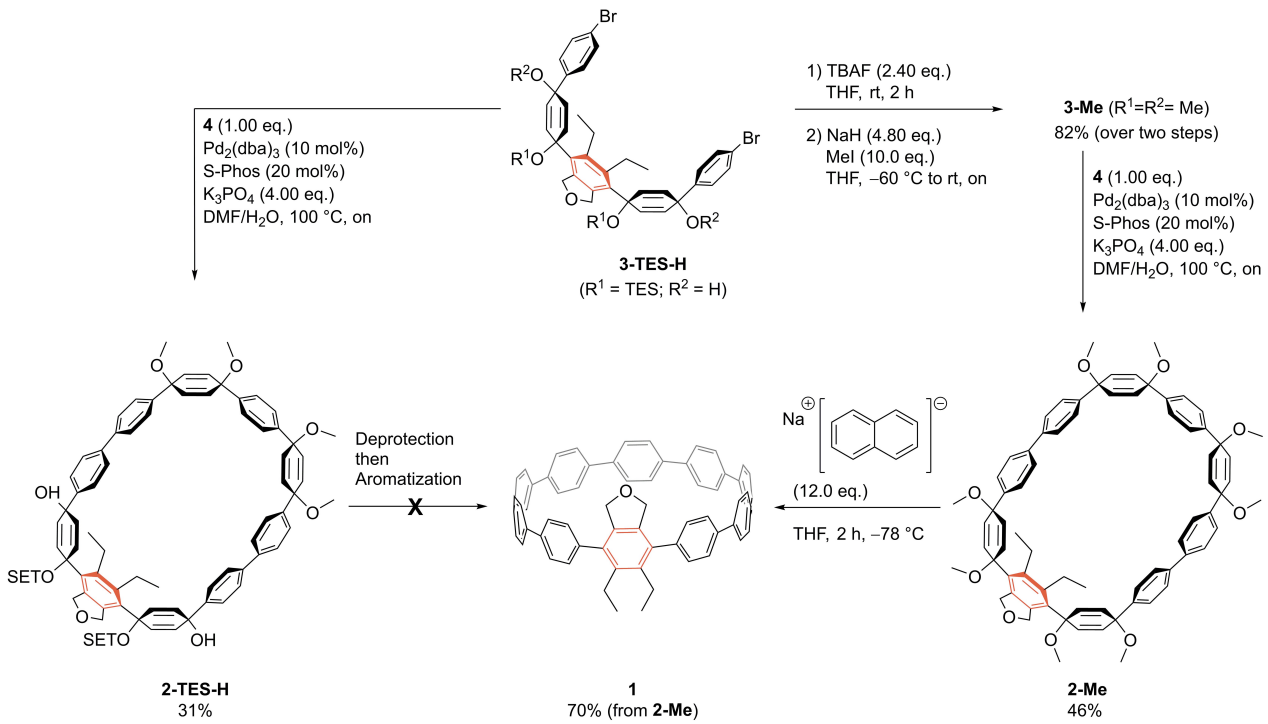

Scheme 3. Completion of the synthesis. The faster synthesis without protection yielded in the desired macrocycle, but not in the targeted CPP (left path), while a de- and reprotection of the five-membered building block **3-TES-H** provided the substituted CPP after a successful macrocyclization (right path).

Research Article
doi.org/10.1002/ejoc.202101357

substituted [8]CPP (0.01 % yield).[8] Especially the critical steps, the macrocyclization and the aromatization have been greatly improved. By using a rigid U-shaped building block, the macrocyclization is significantly enhanced in contrast to the reaction with flexible building blocks. Furthermore, the use of cyclohexadienes proved to be more efficient to aromatize compared to cyclohexanes.[7,27]

Optoelectronic properties

Compound **1** exhibits an absorption maximum at 326 nm, as well as a broad shoulder between 350 and 425 nm (Figure 3), displaying a hypsochromic shift compared to [10]CPP (340 nm). This blue shift can be rationalized by the larger torsion angle in the substituted case resulting in a reduced conjugation. This structural change has been well characterized by *X*-ray analysis for a substituted [8]CPP.[8] The same circumstance leads to a lower extinction coefficient for the substituted CPP **1**. This observation is in a good agreement to other functionalized CPPs.[8,19] The hypsochromic shift ($\Delta\lambda$) in case of the analogous substituted [8]CPP compared to the parent [8]CPP is slightly larger ($\Delta\lambda_{abs}$([8]CPP) = 28 nm) in respect to the here reported [10]CPP ($\Delta\lambda_{abs}$([10]CPP) = 14 nm).[8] CPP **1** has a larger ring size and lower degree of substitution with respect to the reported [8]CPP resulting in a less pronounced variation compared to the parent CPP. The fluorescence spectrum shows two emission maxima at 436 and 458 nm, respectively. The blue shifted maximum exhibits the highest intensity, which can only be observed as a shoulder in the unsubstituted case. According to Tretiak and coworkers these two maxima can be ascribed to vibronic features and accordingly decreased vibrational coupling.[28] Similar to the absorption, the fluorescence is shifted hypsochromically, compared to the unsubstituted case (474 nm). In comparison to the previously reported [8]CPP the aberration in [10]CPP **1** is much less distinct. While the substitution within the [8]CPP led to blue shift in the fluorescence of $\Delta\lambda_{em}$([8]CPP) = 87 nm,[8] it is only $\Delta\lambda_{em}$([10]CPP) - = 16 nm in case of the [10]CPP.

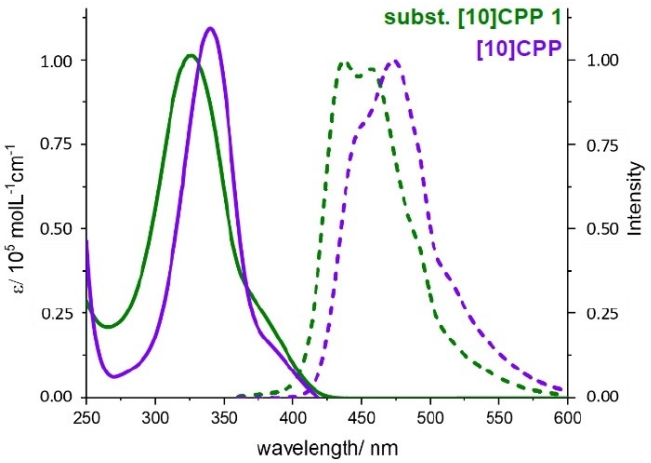

Figure 3. Absorption (solid lines, 10^{-5} M) and emission (dashed lines, 10^{-6} M) spectra of CPP **1** and [10]CPP measured in $CHCl_3$.

Conclusion

In conclusion, a synthesis for a substituted CPP was developed. The synthesis disclosed unexpected issues like a strongly hindered [2 + 2 + 2] cycloaddition of building block **6-Me**, as well as a remarkable stability of diol **3-TES-H** against deprotonation. In the end, all obstacles were overcome and the targeted substituted [10]CPP **1** was obtained in an overall yield of 8 %. In this context the extraordinary high yield of both, the macrocyclization and the aromatization has to be highlighted, which is in contrast to the previously reported synthesis of a diethylphthalane incorporated CPP and other syntheses of substituted nanohoops. With a hypsochromic shift in absorption and fluorescence, as well as a decrease in the extinction, the observed optoelectronic properties are in good agreement with other substituted cycloparaphenylenes.

Experimental Section

General Information

NMR spectroscopy*:* NMR spectra were measured on a Bruker Avance II 200 MHz, Avance II 400 MHz, Avance III 400 MHz HD or Avance III 600 MHz spectrometer at 25 °C if not otherwise noted. As the internal reference, the shifts of the solvent residual peaks were used.[29]

Mass spectrometry: ESI-MS spectra were measured on a Bruker Daltonics Micro TOF LC. The samples were dissolved in methanol. A positive voltage of 4500 V was applied to the capillary and −500 V to the End Plate Offset. The nebulizer was set to 0.4 bar. The dry heater was set to 180 °C and the flow of nitrogen as the dry gas to 4.0 l/min. For measurements in the negative ion mode, a negative voltage of 3000 V was applied, while the other parameters remained the same. For the MALDI-MS measurements a house made MALDI-source was used with 2,5-dihydroxybenzoic acid as the matrix. The mass spectrometer Q-Exactive™ by Thermo Fisher Scientific was connected to the MALDI-source.

Chemicals: The chemicals were purchased from Sigma-Aldrich, Acros Organics, Alfa Aesar, BLD-Pharm and TCI Europe. Anhydrous solvents were purchased from Acros Organics. Deuterated solvents were purchased from Euriso-Top GmbH. Technical grade solvents, used during work-up and purification, were distilled prior to use. Dry THF used for the aromatization step was distilled prior to use to remove the stabilizing agent. The unsubstituted diboronic ester **4** was synthesized according to a published synthesis.[23]

Column chromatography: Flash column chromatography was carried out with Silica 60 M (0.04–0.063 mm) from Macherey-Nagel GmbH & Co. KG. Thin layer chromatography was carried out on Polygram® SIL G/UV254 from Macherey-Nagel GmbH & Co. KG.

Melting point determination: Melting points were determined on a M5000 melting point meter from A. KRÜSS Optronic GmbH, Germany. A heating rate of 1 °C min^{-1} and a resolution of 0.1 °C were used, with an accuracy of ±0.3 °C (25–200 °C) and ±0.5 °C (200–400 °C).

Microwave reactions: Microwave reactions were performed in a Discoverer SP Activent® microwave reactor by CEM.

UV-Vis spectroscopy: Solvents for UV/Vis spectroscopy were purchased from Merck or Chemsolute (Uvasol® or HPLC quality). The measurements were carried out with a SPECORD® 200 PLUS spectrophotometer equipped with two automatic eight-fold cell changers and a Peltier element thermostat system (0.1 °C accuracy) by Analytik Jena.

Fluorescence spectroscopy*:* Solvents for UV/Vis spectroscopy were purchased from Merck or Chemsolute (Uvasol® or HPLC quality). The measurements were carried out with a FP-8300 fluorescence spectrometer from Jasco. The sample was irradiated with a Xe-lamp. Excitation and emission bandwidth were set to 2.5 nm.

Synthetic procedures

Synthesis of diketone 8*:* Propargyl ether **9** (84% in toluene, 3.49 g, 31.1 mmol, 1.00 eq.) and 200 ml dry THF were placed in a flame-dried flask and cooled to −78 °C. A solution of *n*-BuLi (1.6 M in hexanes, 46.0 ml, 73.6 mmol, 2.37 eq.) was added within 30 min and the resulting suspension was stirred for another 30 min. In a second flask, freshly recrystallized 1,4-benzoquinone (11.7 g, 109 mmol, 3.52 eq.) was dissolved in 150 ml dry THF. After cooling to −40 °C, the benzoquinone solution was transferred to the other flask *via* a transfer cannula. The residue was dissolved in 40 ml dry THF and again transferred to the reaction mixture, which was then stirred at −40 °C overnight. To quench the reaction, 80 ml saturated aq. NH_4Cl solution were added and the mixture was subsequently allowed to reach rt. The organic phase was extracted with ethyl acetate (3×150 ml) washed with brine (150 ml), dried over $MgSO_4$, filtered and concentrated under reduced pressure. The crude product was dissolved in ethyl acetate, filtered through Celite© and concentrated at reduced pressure. Afterwards, it was purified by flash silica column chromatography with ethyl acetate/cyclohexane as eluent (1:1 to 3:1) to obtain an off-white solid (5.14 g, 16.6 mmol, 53%). ^{1}H NMR (400 MHz, DMSO-d_6) δ 7.01–6.93 (m, 4H), 6.72 (s, 2H), 6.16–6.09 (m, 4H), 4.23 ppm (s, 4H). ^{13}C NMR (101 MHz, DMSO-d_6) δ 184.4 (2 C), 148.4 (4 C), 125.8 (4 C), 84.4 (2 C), 80.2 (2 C), 61.2 (2 C), 56.4 ppm (2 C). HRMS (ESI): calc. for $[C_{18}H_{14}NaO_5]^+$: $[M+Na]^+$ 333.0733, found 333.0731. MP > 115 °C (dec.).

Synthesis of dialkyne 6-Me: Diketone **8** (0.620 g, 2.00 mmol, 1.00 eq.) was placed in a flame-dried flask, dissolved in 40 ml dry THF and cooled to −70 °C. Sodium hydride (60% in mineral oil, 239 mg, 5.98 mmol, 2.99 eq.) was added and the mixture was stirred for 30 min. In a second flame-dried flask, 1,4-dibromobenzene (**10**) (1.94 g, 8.06 mmol, 4.03 eq.) was dissolved in 50 ml dry THF and subsequent cooled to −70 °C. *n*-BuLi (5.50 ml, 1.6 M in hexanes, 8.80 mmol, 4.40 eq.) was added and the resulting suspension was stirred for 30 min. Afterwards, the suspension containing lithiated bromobenzene was transferred to the diketone mixture *via* a transfer cannula within 10 min. The reaction mixture was stirred and allowed to reach rt overnight. The reaction mixture was cooled to −55 °C and 80 ml half-saturated aq. NH_4Cl solution were added to quench the reaction. After reaching rt, the organic phase was extracted with ethyl acetate (2×75 ml). The combined organic phases were washed with brine (75 ml), dried over $MgSO_4$, filtered and the volatiles were removed at reduced pressure. Cyclohexane (5 ml) was added to dissolve impurities, subsequently removed with a pipette and the solid was dried under vacuum. One third of the crude product was redissolved in 35 ml dry THF and cooled to −60 °C. Sodium hydride (105 mg, 60% in mineral oil, 2.65 mmol, 4.11 eq.) was added and the mixture was stirred for 30 min. Meanwhile, 15-crown-5 (0.55 ml, 2.75 mmol, 4.26 eq.) was dissolved in 5 ml dry THF and subsequently added to the reaction mixture at −55 °C. After stirring for 30 min, iodomethane (800 µl, 12.9 mmol, 19.9 eq.) was added at −50 °C. The reaction mixture was allowed to reach rt and was stirred overnight. Water (20 ml) was added to quench the reaction. The organic phase was extracted with ethyl acetate (2×20 ml) and the combined organic phases were washed with brine (20 ml), dried with $MgSO_4$, filtered and the volatiles were removed at reduced pressure. The product was purified twice by alumina oxide (neutral) column chromatography with cyclohexane/ethyl acetate/DCM (1st column: 10:1:1 to 8:1:1, 2nd column: 20:1:1 to 5:1:1) as eluent to obtain the product **6-Me** as a yellowish waxy solid (249 mg; 0.366 mmol, 56%). ^{1}H NMR (400 MHz, THF-d_8) δ 7.46–7.41 (m, 4H), 7.37–7.33 (m, 4H), 6.20–6.14 (m, 4H), 5.84–5.78 (m, 4H), 4.31 (s, 4H), 3.36 (s, 6H), 3.29 ppm (s, 6H). ^{13}C NMR (101 MHz, THF-d_8) δ 143.8 (2 C), 133.8 (4 C), 132.0 (4 C), 131.0 (4 C), 128.7 (4 C), 121.9 (2 C), 86.6 (2 C), 82.2 (2 C), 75.7 (2 C), 67.6 (2 C), 57.0 (2 C), 52.2 (2 C), 51.9 ppm (2 C). HRMS (ESI): calc. for $[C_{34}H_{32}Br_2O_5Na]^+$: $[M+Na]^+$ 701.0508, found 701.0506. MP Due to its texture, no melting point could be determined.

Synthesis of the TES-protected diketone 8-TES*:* Diketone **8** (318 mg, 1.02 mmol, 1.00 eq.) and imidazole (273 mg, 4.01 mmol, 3.91 eq.) were added to a flame-dried round bottom flask containing dry DMF (20 ml). The mixture was stirred until all solids were dissolved and subsequently TESCl (400 µl, 2.36 mmol, 2.30 eq.) was added dropwise to the stirring solution. After the complete addition, the resulting solution was stirred at rt overnight. Water (15 ml) was added to the crude reaction, which was then extracted with DCM (3×15 ml). The combined organic phases were washed with water (3×15 ml), brine (15 ml), dried over $MgSO_4$, filtered and concentrated at reduced pressure. The product was obtained as a yellow oil (527 mg, 0.980 mmol, 95%). ^{1}H NMR (400 MHz, DMSO-d_6) δ 7.00–6.95 (m, 4H), 6.19–6.14 (m, 4H), 4.27 (s, 5H), 0.92 (t, ^3J= 7.9 Hz, 18H), 0.65 ppm (q, ^3J=7.9 Hz, 12H). ^{13}C-NMR (101 MHz, DMSO-d_6) δ 184.2 (2 C), 147.8 (4 C), 126.1 (4 C), 83.8 (2 C), 81.8 (2 C), 63.4 (2 C), 56.5 (2 C), 6.8 (6 C), 5.7 ppm (6 C). HRMS (ESI): calc. for $[C_{30}H_{42}O_5Si_2Na]^+$: $[M+Na]^+$ 561.2463, found 561.2464.

Synthesis of 3-membered building block 5-TES through [2+2+2] cycloaddition*:* Dialkyne **8-TES** (527 mg, 0.978 mmol, 1.00 eq.), 3-hexyne (**7**) (2.25 ml, 19.6 mmol, 20.0 eq.), dry *i*-PrOH (35 ml) and dry THF (35 ml) were placed in a flame dried Schlenk tube under N_2. $[Rh(PPh_3)_3Cl]$ (67.8 mg, 73.3 µmol, 7.50 mol%) was added and the reaction mixture was heated to 50 °C overnight. Water (70 ml) was added and the aqueous phase was extracted with DCM (3×70 ml). The combined org. layers were washed with water (2×70 ml), brine (70 ml) and dried with $MgSO_4$. The solid was removed by filtration and the volatiles were evaporated at reduced pressure. The crude product was purified by flash silica chromatography with toluene/ethyl acetate/NEt_3 (10:1; 1% NEt_3) as eluent The product **5-TES** was obtained as a white crystalline solid (429 mg, 0.691 mmol, 71%). In case the column chromatography does not liberate the pure product, it can be further purified by recrystallization from *n*-pentane. ^{1}H NMR (400 MHz, $CDCl_3$) δ 7.02–6.96 (m, 4H), 6.31–6.26 (m, 4H), 5.21 (s, 4H), 2.61 (q, ^3J=8.0 Hz, 4H), 0.97–0.89 (m, 24H), 0.66 ppm (q, ^3J=8.6, 7.9 Hz, 12H). ^{13}C NMR (101 MHz, $CDCl_3$) δ 185.6 (2 C), 150.7 (4 C), 141.2 (2 C), 138.9 (2 C), 134.4 (2 C), 127.5 (4 C), 73.8 (2 C), 73.4 (2 C), 21.2 (2 C), 17.6 (2 C), 7.1 (6 C), 6.3 ppm (6 C). HRMS (ESI): calc. for $[C_{36}H_{52}O_5Si_2Na]^+$: $[M+Na]^+$ 643.3245, found 643.3247. MP 97–98 °C.

Synthesis of 5-membered building block 3-TES-H: 1,4-Dibromobenzene (**10**) (733 mg, 3.04 mmol, 3.79 eq.) was placed in a flame-dried Schlenk tube and subsequently dissolved in dry THF (30 ml). After cooling to −78 °C, *n*-BuLi (2.20 ml, 1.6 M in hexanes, 3.52 mmol, 4.37 eq.) was added. The suspension was stirred for 30 min while reaching −50 °C. At this temperature diketone **5-TES** (498 mg, 0.802 mmol, 1.00 eq.) was added and the reaction mixture was allowed to reach rt overnight. The reaction mixture was cooled

to −20 °C and half-saturated aq. NH_4Cl-solution (30 ml) was added. The mixture was allowed to reach rt and the organic phase was extracted with DCM (3×20 ml). The combined organic phases were washed with water (3×50 ml) and brine (50 ml). Subsequently, the organic phase was dried with $MgSO_4$, filtered and the volatiles were evaporated. A purification by flash silica chromatography with cyclohexane/DCM/ethyl acetate/ NEt_3 (20:1:1 to 10:1:1 with 1% NEt_3) as eluent afforded the product **3-TES-H** as a white crystalline solid (645 mg, 0.690 mmol, 86%). *Note gram scale:* On a 4.9 mmol scale, 2.9 g product were obtained (65%). ^{1}H NMR (400 MHz, DMSO-d_6) δ 7.55–7.48 (m, 4H), 7.38–7.33 (m, 4H), 6.13–6.05 (m, 8H), 5.83 (s, 2H), 4.80 (s, 4H), 2.48–2.36 (m, 4H), 0.90 (t, ^3J = 7.8 Hz, 18H), 0.75–0.62 ppm (m, 18H). ^{13}C-NMR (101 MHz, DMSO-d_6) δ 145.0 (2 C), 140.8 (2 C), 137.5 (2 C), 136.8 (2 C), 131.4 (2 C), 130.8 (4 C), 130.5 (2 C), 128.3 (4 C), 120.4 (2 C), 72.6 (4 C), 66.8 (4 C), 26.3 (2 C), 20.8 (2 C), 17.3 (2 C), 7.0 (6 C), 5.6 ppm (6 C). HRMS (MALDI): calc. for $[C_{48}H_{62}Br_2O_5Si_2Na]^+$: $[M+Na]^+$ 955.2395, found 955.2404. MP 106–107 °C

Synthesis of OH-OTES-OMe-[10]macrocycle 2-TES-H: Tetra-substituted [5]building block **3-TES-H** (310 mg, 332 μmol, 1.00 eq.) and unsubstituted [5]building block **4** (251 mg, 319 μmol, 1.00 eq.) were dissolved in 80 ml DMF and 10 ml H_2O and subsequently degassed with N_2 (15 min). $Pd_2(dba)_3$ (31 mg, 33 μmol, 10 mol%), SPhos (28 mg, 67 μmol, 20 mol%) and $K_3PO_4 \times H_2O$ (310 mg, 1.28 mmol, 3.85 eq.) were added and the reaction mixture was heated to 100 °C overnight. The reaction mixture was filtered through a plug of Celite® and water (100 ml) was added. The organic phase was extracted with DCM (3×100 ml), washed with water (6×100 ml), dried with $MgSO_4$, filtered and concentrated at reduced pressure. The crude product was purified by silica column chromatography with cyclohexane/DCM/EtOAc (10:1:1 to 5:1:1) and toluene:DCM:EtOAc (5:1:1 to 4:1:1) as eluent to afford a white solid (130 mg, 102 μmol, 31%). ^{1}H NMR (400 MHz, C_6D_6): δ 7.82 (s, 4H), 7.60–7.57 (m, 4H), 7.46–7.42 (m, 4H), 7.41–7.36 (m, 8H), 6.13–6.08 (m, 4H), 6.02–5.97 (m, 4H), 5.97–5.93 (m, 4H), 5.92–5.87 (m, 4H), 5.66 (s, 4H), 3.33 (s, 6H), 3.28 (s, 6H), 2.69–2.53 (m, 4H), 1.01 (t, ^3J = 7.8 Hz, 18H), 0.88–0.72 ppm (m, 18H). ^{13}C NMR (101 MHz, C_6D_6) δ 144.2 (2 C), 143.8 (2 C), 142.8 (2 C), 141.4 (2 C), 140.8 (2 C), 140.1 (2 C), 139.1 (2 C), 137.9 (2 C), 133.5 (2 C), 133.5 (2 C), 133.4 (2 C), 130.2 (2 C), 127.6 (4 C), 127.2 (4 C), 127.2 (4 C), 127.0 (4 C), 126.8 (4 C), 74.5 (2 C), 74.4 (4 C), 74.3 (4 C), 73.7 (4 C), 68.5 (4 C), 51.8 (4 C, overlaying signals), 22.1 (2 C), 18.0 (2 C), 7.4 (6 C), 6.8 ppm (6 C). HRMS(ESI): calc. for $[C_{82}H_{94}O_9Si_2Na]^+$: $[M+Na]^+$ 1301.6328, found 1301.6329. MP > 160 °C (dec.)

Synthesis of all-OMe-5-membered building block 3-Me: Building block **3-TES-H** (1.00 g, 1.07 mmol, 1.00 eq.) was dissolved in 20 ml THF and TBAF (2.60 ml, 1.0 M in THF, 2.60 mmol, 2.43 eq.) was added. The mixture was allowed to stir for 2 h at rt before water (20 ml) was added. The THF was evaporated whereat a white solid was formed, which was filtered off and washed with water and *n*-pentane to give the tetraalcohol as a white solid. The crude tetraalcohol was redissolved in dry THF (55 ml) and cooled to −60 °C. NaH (186 mg; 60% in mineral oil, 4.64 mmol, 4.80 eq.) was added and the reaction mixture was stirred for 30 min. MeI (0.61 ml, 9.67 mmol, 10.0 eq.) was added and the reaction was allowed to reach rt overnight. The reaction was quenched by adding water (50 ml). The organic phase was extracted with DCM (3×50 ml), washed with water (3×100 ml), brine (50 ml), dried with $MgSO_4$, filtrated and the volatiles were removed at reduced pressure. Crude product was washed with *n*-pentane to give the product as a white solid (670 mg, 0.879 mmol, 82%). ^{1}H NMR (400 MHz, $CDCl_3$) δ 7.52–7.45 (m, 4H), 7.35–7.28 (m, 4H), 6.30–6.19 (m, 4H), 6.16–6.07 (m, 4H), 5.04 (s, 4H), 3.29 (s, 6H), 3.24 (s, 6H), 2.58–2.45 (m, 4H), 0.79 ppm (t, ^3J = 7.2 Hz, 6H). ^{13}C NMR (101 MHz, $CDCl_3$) δ 141.6 (2 C), 141.4 (2 C), 138.4 (2 C), 136.4 (2 C), 132.8 (4 C), 131.7 (4 C), 131.6 (4 C), 128.5 (4 C), 122.2 (2 C), 75.4 (2 C), 73.7 (2 C), 73.3 (2 C), 51.8 (2 C), 49.8 (2 C) 21.7 (2 C), 17.5 ppm (2 C). HRMS (ESI): calc. for $[C_{40}H_{42}Br_2O_5Na]^+$: $[M+Na]^+$ 783.1291, found 783.1294. MP 142–144 °C

Synthesis of all-OMe-[10]macrocycle 2-Me*:* Tetrasubstituted [5]building block **3-Me** (254 mg, 333 μmol, 1.00 eq.) and unsubstituted building block **4** (252 mg, 332 μmol, 1.00 eq.) were dissolved in 80 ml DMF and 10 ml H_2O and subsequently degassed with N_2 (15 min). $Pd_2(dba)_3$ (31.5 mg, 33.4 μmol, 10 mol%), SPhos (28.0 mg, 66.6 μmol, 20.0 mol%) and $K_3PO_4 \times H_2O$ (323 mg, 1.33 mmol, 4.00 eq.) were added and the reaction mixture was heated to 100 °C overnight. The reaction mixture was filtered through a plug of Celite® and water (100 ml) was added. The organic phase was extracted with DCM (3×100 ml), washed with water (6×100 ml), dried with $MgSO_4$, filtered and concentrated at reduced pressure. The crude product was purified by silica column chromatography with cyclohexane/DCM/EtOAc (10:5:3) as eluent. Washing with *n*-pentane afforded the product as a white solid (169 mg, 153 μmol, 46%). ^{1}H NMR (400 MHz, CD_2Cl_2) δ 7.57–7.51 (m, 8H), 7.50–7.43 (m, 8H), 7.42 (s, 4H), 6.34–6.28 (m, 4H), 6.13–6.03 (m, 12H), 5.07 (s, 4H), 3.42–3.38 (m, 2 overlaying singlets, 12H), 3.35 (s, 6H), 3.27 (s, 6H), 2.36–2.21 (m, 4H), 0.56 ppm (*t*, ^3J = 7.2 Hz, 4H). ^{13}C NMR (101 MHz, CD_2Cl_2) δ 143.3 (2 C), 143.3 (2 C), 141.5 (2 C), 140.8 (2 C), 140.0 (2 C), 139.7 (2 C), 138.4 (2 C), 136.0 (2 C), 133.2 (2 C), 133.0 (2 C), 132.6 (2 C), 132.0 (2 C), 127.4 (4 C), 127.0 (4 C), 126.6 (4 C), 126.5 (4 C), 126.0 (4 C), 75.9 (4 C), 74.0 (4 C), 74.0 (4 C), 73.7 (4 C), 73.6 (2 C), 51.7 (4 C, 2 overlaying signals), 51.6 (2 C), 49.4 (2 C), 21.7 (2 C), 17.3 ppm (2 C). HRMS (APCI): calc. for $[C_{74}H_{75}O_9]^+$: $[M+H]^+$ 1107.5406, found 1107.5405. MP > 190 °C (dec.)

Sodium naphthalenide: Naphthalene (1.92 g, 15.0 mmol, 1.00 eq.) was placed in a flame died Schlenk tube and dry stabilizer-free THF (50 ml) was added. Sodium metal (517 mg, 22.5 mmol, 1.50 eq.) was added in small portions resulting in a deep green suspension, which was stirred at rt overnight. The metal residues were removed by filtration through a glass fiber pad and the sodium naphthalenide concentration of the obtained solution was determined by threefold titration of menthol.

Synthesis of substituted [10]CPP 1: Macrocycle **2-Me** (70.0 mg, 63.2 μmol, 1.00 eq.) and dry stabilizer-free THF (30 ml) were placed in a nitrogen filled flame dried Schlenk tube and cooled to −78 °C. Freshly prepared sodium naphthalenide (2.62 ml, 0.290 M in THF, 0.760 mmol, 12.0 eq.) was added and the reaction mixture was stirred for 2 h at that temperature. Then, I_2 (15 ml, 1 M in THF, 15 mmol) was added and the reaction was allowed to reach rt. Saturated aq. sodium thiosulfate solution was added to remove the excess of I_2. Water (60 ml) was added and the organic phase was extracted with DCM (3×60 ml). The combined organic layer was washed with brine (60 ml) and dried over $MgSO_4$, filtrated and the volatiles were removed under reduced pressure. The crude product was loaded on a pad of alumina oxide (neutral), whereat remaining naphthalene was removed with cyclohexane:DCM 1:1. The product was subsequently eluted with DCM and obtained as a yellow fluorescent solid (38.0 mg, 44.2 μmol, 70%). ^{1}H NMR (400 MHz, CD_2Cl_2): δ 7.64–7.54 (m, 26H), 7.54–7.50 (m, 4H), 7.17–7.13 (m, 4H), 4.01 (s, 4H), 3.04 (q, ^3J = 7.4 Hz, 4H), 1.24 ppm (t, ^3J = 7.4 Hz, 6H). ^{13}C NMR (101 MHz, CD_2Cl_2): δ 140.1 (2 C), 139.4 (2 C), 139.3 (2 C), 139.2 (2 C), 138.8 (4 C), 138.7 (2 C), 138.6 (2 C), 138.6 (2 C), 138.5 (4 C, 2 overlaying signals), 135.9 (2 C), 130.6 (4 C), 128.0 (4 C), 127.9 (4 C), 127.83 (4 C), 127.76 (8 C, 2 overlaying signals), 127.72 (4 C), 127.66 (4 C), 127.4 (4 C, 74.6 (2 C), 23.9 (2 C), 17.0 ppm (2 C). Digits were added to show the difference in the chemical shift. HRMS (APCI): calc. for $[C_{66}H_{51}O]^+$: $[M+H]^+$ 859.3935, found 859.3933. MP > 250 °C (dec.)

Acknowledgements

The authors thank Katharina Heinrich, Domenic Dreisbach and Prof. Bernhard Spengler for the MALDI-MS measurements, Dr. Heike Hausmann for NMR measurements and Dr. Jonathan Becker for X-ray diffraction measurements. Furthermore, the authors thank Jan H. Griwatz and Sebastian Beeck for inspiration and fruitful discussions. Open Access funding enabled and organized by Projekt DEAL.

Conflict of Interest

The authors declare no conflict of interest.

Data Availability Statement

The data that support the findings of this study are available in the supplementary material of this article.

Keywords: Cyclotrimerization · Fluorescence · Macrocycles · Nanostructures · Synthesis design

[1] a) S. E. Lewis, *Chem. Soc. Rev.* **2015**, *44*, 2221–2304; b) Y. Segawa, A. Yagi, K. Matsui, K. Itami, *Angew. Chem. Int. Ed.* **2016**, *55*, 5136–5158; *Angew. Chem.* **2016**, *128*, 5222–5245; c) A.-F. Tran-Van, H. A. Wegner, *Beilstein J. Nanotechnol.* **2014**, *5*, 1320–1333; d) Y. Xu, M. von Delius, *Angew. Chem. Int. Ed.* **2020**, *59*, 559–573; *Angew. Chem.* **2020**, *132*, 567–582.

[2] R. Jasti, J. Bhattacharjee, J. B. Neaton, C. R. Bertozzi, *J. Am. Chem. Soc.* **2008**, *130*, 17646–17647.

[3] a) M. Fujitsuka, D. W. Cho, T. Iwamoto, S. Yamago, T. Majima, *Phys. Chem. Chem. Phys.* **2012**, *14*, 14585–14588; b) E. R. Darzi, R. Jasti, *Chem. Soc. Rev.* **2015**, *44*, 6401–6410; c) T. Iwamoto, Y. Watanabe, H. Takaya, T. Haino, N. Yasuda, S. Yamago, *Chem. Eur. J.* **2013**, *19*, 14061–14068; d) Y. Nakanishi, H. Omachi, S. Matsuura, Y. Miyata, R. Kitaura, Y. Segawa, K. Itami, H. Shinohara, *Angew. Chem. Int. Ed.* **2014**, *53*, 3102–3106; *Angew. Chem.* **2014**, *126*, 3166–3170; e) N. Grabicki, K. T. D. Nguyen, S. Weidner, O. Dumele, *Angew. Chem. Int. Ed.* **2021**, *60*, 14909–14914.

[4] a) Omachi, Y. Yamamoto, J. Bouffard, K. Itami, *Angew. Chem. Int. Ed.* **2009**, *48*, 6112–6116; *Angew. Chem.* **2009**, *121*, 6228–6232; b) S. Yamago, Y. Watanabe, T. Iwamoto, *Angew. Chem. Int. Ed.* **2010**, *49*, 757–759; *Angew. Chem.* **2010**, *122*, 769–771.

[5] F. E. Golling, M. Quernheim, M. Wagner, T. Nishiuchi, K. Müllen, *Angew. Chem. Int. Ed.* **2014**, *126*, 1551–1554.

[6] S. Hashimoto, E. Kayahara, Y. Mizuhata, N. Tokitoh, K. Takeuchi, F. Ozawa, S. Yamago, *Org. Lett.* **2018**, *20*, 5973–5976.

[7] Y. Miyauchi, K. Johmoto, N. Yasuda, H. Uekusa, S. Fujii, M. Kiguchi, H. Ito, K. Itami, K. Tanaka, *Chem. Eur. J.* **2015**, *21*, 18900–18904.

[8] A.-F. Tran-Van, E. Huxol, J. M. Basler, M. Neuburger, J.-J. Adjizian, C. P. Ewels, H. A. Wegner, *Org. Lett.* **2014**, *16*, 1594–1597.

[9] E. Kayahara, M. Nakano, L. Sun, K. Ishida, S. Yamago, *Chem. Asian J.* **2020**, *15*, 2451–2455.

[10] E. Kayahara, V. K. Patel, A. Mercier, E. P. Kündig, S. Yamago, *Angew. Chem. Int. Ed.* **2016**, *128*, 310–314.

[11] E. Kayahara, R. Qu, S. Yamago, *Angew. Chem. Int. Ed.* **2017**, *56*, 10428–10432; *Angew. Chem.* **2017**, *129*, 10564–10568.

[12] N. Kubota, Y. Segawa, K. Itami, *J. Am. Chem. Soc.* **2015**, *137*, 1356–1361.

[13] E. Kayahara, L. Sun, H. Onishi, K. Suzuki, T. Fukushima, A. Sawada, H. Kaji, S. Yamago, *J. Am. Chem. Soc.* **2017**, *139*, 18480–18483.

[14] E. J. Leonhardt, J. M. van Raden, D. Miller, L. N. Zakharov, B. Alemán, R. Jasti, *Nano Lett.* **2018**, *18*, 7991–7997.

[15] B. M. White, Y. Zhao, T. E. Kawashima, B. P. Branchaud, M. D. Pluth, R. Jasti, *ACS Cent. Sci.* **2018**, *4*, 1173–1178.

[16] a) K. Ypsilantis, T. Tsolis, A. Garoufis, *Inorg. Chem. Commun.* **2021**, *134*, 108992; b) F. E. Golling, S. Osella, M. Quernheim, M. Wagner, D. Beljonne, K. Müllen, *Chem. Sci.* **2015**, *6*, 7072–7078; c) P. Della Sala, C. Talotta, M. de Rosa, A. Soriente, S. Geremia, N. Hickey, P. Neri, C. Gaeta, *J. Org. Chem.* **2019**, *84*, 9489–9496; d) D. Lu, G. Zhuang, H. Jia, J. Wang, Q. Huang, S. Cui, P. Du, *Org. Chem. Front.* **2018**, *5*, 1446–1451; e) S. Cui, G. Zhuang, J. Wang, Q. Huang, S. Wang, P. Du, *Org. Chem. Front.* **2019**, *6*, 1885–1890; f) Y. Xu, B. Wang, R. Kaur, M. B. Minameyer, M. Bothe, T. Drewello, D. M. Guldi, M. von Delius, *Angew. Chem. Int. Ed.* **2018**, *57*, 11549–11553; *Angew. Chem.* **2018**, *130*, 11723–11727; g) Y. Kuroda, Y. Sakamoto, T. Suzuki, E. Kayahara, S. Yamago, *J. Org. Chem.* **2016**, *81*, 3356–3363; h) E. Kayahara, X. Zhai, S. Yamago, *Can. J. Chem.* **2017**, *95*, 351–356; i) K. Itami, H. Shudo, M. Kuwayama, M. Shimasaki, T. Nishihara, Y. Takeda, T. Kuwabara, A. Yagi, Y. Segawa, **2021**, ChemRxiv preprint DOI: 10.33774/chemrxiv-2021-7kd63; j) T. C. Lovell, Z. R. Garrison, R. Jasti, *Angew. Chem. Int. Ed.* **2020**, *59*, 14363–14367; *Angew. Chem.* **2020**, *132*, 14469–14473.

[17] J. Xia, M. R. Golder, M. E. Foster, B. M. Wong, R. Jasti, *J. Am. Chem. Soc.* **2012**, *134*, 19709–19715.

[18] N. Hayase, Y. Miyauchi, Y. Aida, H. Sugiyama, H. Uekusa, Y. Shibata, K. Tanaka, *Org. Lett.* **2017**, *19*, 2993–2996.

[19] N. Hayase, H. Sugiyama, H. Uekusa, Y. Shibata, K. Tanaka, *Org. Lett.* **2019**, *21*, 3895–3899.

[20] C. Huang, Y. Huang, N. G. Akhmedov, B. V. Popp, J. L. Petersen, K. K. Wang, *Org. Lett.* **2014**, *16*, 2672–2675.

[21] a) G. Domínguez, J. Pérez-Castells, *Chem. Soc. Rev.* **2011**, *40*, 3430–3444; b) G. Nishida, N. Suzuki, K. Noguchi, K. Tanaka, *Org. Lett.* **2006**, *8*, 3489–3492.

[22] S. Nishigaki, Y. Shibata, A. Nakajima, H. Okajima, Y. Masumoto, T. Osawa, A. Muranaka, H. Sugiyama, A. Horikawa, H. Uekusa, H. Koshino, M. Uchiyama, A. Sakamoto, K. Tanaka, *J. Am. Chem. Soc.* **2019**, *141*, 14955–14960.

[23] J. Xia, J. W. Bacon, R. Jasti, *Chem. Sci.* **2012**, *3*, 3018–3021.

[24] T. J. Sisto, M. R. Golder, E. S. Hirst, R. Jasti, *J. Am. Chem. Soc.* **2011**, *133*, 15800–15802.

[25] M. Wächter, *Tabellenbuch der Chemie. Daten zur Analytik, Laborpraxis und Theorie*, Wiley-VCH, Weinheim, **2012**.

[26] a) V. K. Patel, E. Kayahara, S. Yamago, *Eur. J. Org. Chem.* **2015**, *21*, 5742–5749; b) Y. Yang, O. Blacque, S. Sato, M. Juríček, *Angew. Chem. Int. Ed.* **2021**, *133*, 13641–13647.

[27] E. R. Darzi, T. J. Sisto, R. Jasti, *J. Org. Chem.* **2012**, *77*, 6624–6628.

[28] L. Adamska, I. Nayyar, H. Chen, A. K. Swan, N. Oldani, S. Fernandez-Alberti, M. R. Golder, R. Jasti, S. K. Doorn, S. Tretiak, *Nano Lett.* **2014**, *14*, 6539–6546.

[29] G. R. Fulmer, A. J. M. Miller, N. H. Sherden, H. E. Gottlieb, A. Nudelman, B. M. Stoltz, J. E. Bercaw, K. I. Goldberg, *Organometallics* **2010**, *29*, 2176–2179.

Manuscript received: November 8, 2021
Revised manuscript received: December 10, 2021
Accepted manuscript online: December 15, 2021